

## Supplemental material

Mijailovich et al., <https://doi.org/10.1085/jgp.201812165>

### Strain-dependent state transition rates in the three-state actomyosin cycle

To quantitatively assess the effect of ancillary proteins titin and nebulin without loss of generality, we considered a minimal three-state model that includes a swinging lever arm step or power stroke, similar to that proposed by Duke (1999) and Daniel et al. (1998), and includes one detached myosin state (M·ADP·Pi), two attached myosin states (weakly bound, A·M·ADP·Pi), and a state strongly bound to actin after Pi release (A·M·ADP).

The functions for the free energy of the three states in their simplest form, accounting for the cross-bridge distortion only in the axial direction and after setting the unbound state energy 0, are defined as (Duke, 1999)

$$G_1 = 0, \quad (\text{S1a})$$

$$G_2 = \frac{(\Delta G_{\text{bind}} + \frac{\kappa x^2}{2})}{k_B T}, \quad (\text{S1b})$$

$$G_3 = \frac{[\Delta G_{\text{bind}} + \Delta G_{\text{stroke}} + \kappa \frac{(x+d)^2}{2}]}{k_B T}, \quad (\text{S1c})$$

where  $\Delta G_{\text{bind}} < 0$  is reduction in free energy due to myosin binding to actin,  $\Delta G_{\text{stroke}} < 0$  is a large (negative) change in chemical free energy associated with Pi release,  $\kappa$  is the elasticity of the cross-bridges in pN/nm,  $x$  is the cross-bridge (axial) displacement from its unstrained position,  $k_B$  is the Boltzmann constant,  $T$  is absolute temperature in °K, and  $d$  is displacement of the lever arm after carrying out the power stroke, i.e., the length of the power stroke in nanometers. In the above relations, the energy of azimuthal movements is not directly taken into account but they are incorporated into the azimuthal weight factors described above.

For myosin binding to actin, the strain-dependent rate in quadratic form is derived from a Langevin type of equation balancing thermal fluctuations of the detached myosin molecule, elastic restoring, and inertial and viscous drag forces (Kramers, 1940; Papoulis, 1991; Hunt et al., 1994; Daniel et al., 1998):

$$k_{12}(x) = k_{\text{bind}} e^{\frac{-\kappa x^2}{2k_B T}}, \quad (\text{S2a})$$

where  $k_{\text{bind}}$  is the overall binding rate of M·ADP·Pi to actin. The reverse reaction occurs at a constant rate

$$k_{21} = k_{\text{unbind}} = k_{\text{bind}} e^{\frac{\Delta G_{\text{bind}}}{k_B T}},$$

where  $\Delta G_{\text{bind}} < 0$  is reduction in energy due to myosin binding to actin.

The transitions between the two attached states A·M·ADP·Pi and A·M·ADP are rapid. The forward/backward reactions are assumed to be in dynamic equilibrium, where Pi release is accompanied by a large change in chemical free energy:

$$K_{23}(x) \equiv \frac{k_{23}(x)}{k_{32}(x)} = e^{\frac{[\Delta G_{\text{stroke}} + \kappa d^2 (\frac{x}{d} + \frac{1}{2})]}{k_B T}}. \quad (\text{S2b})$$

Because the exponential forms of the forward and backward rate constants can reach huge values and cause numerical problems in calculating the transition probabilities, for convenience we capped the maximums of forward and backward constants as described in Smith and Mijailovich (2008) and Mijailovich et al. (2016).

For the strain-dependent ADP release (i.e., A·M·ADP → A·M), the difference between the initial and final strain energies gives the forward rate as

$$k_{31}(x) = k_{\text{ADP}}^0 e^{-\left[ \frac{\kappa d d (\frac{x}{d} + 1 + \frac{\delta}{2d})}{k_B T} \right]}, \quad (\text{S2c})$$

where  $\delta$  is the displacement that the lever arm must move to open the nucleotide pocket and allow ADP release, and  $k_{\text{ADP}}^0$  is the rate of ADP release when the elastic element is relaxed. ATP binding is much faster than the reverse rate  $k_{13}$ , and thus any strain dependence due to the conformational change has almost no effect. It is therefore reasonable to take  $k_{13}$  to be small and constant.

### Calcium concentration dependence of Tnl interaction with actin and calcium sensitivity of force generation

The calcium sensitivity of force generation can be determined from the force-pCa relations obtained from MUSICO simulations for specific effect from, for example, change of distribution of thin filament lengths from WT to Neb-KO, changes in cross-bridge cycling

kinetics, or changes in titin-based passive force. The thin filament regulation implemented in MUSICO contains the kinetics of calcium binding to TnC and associated change in affinity of TnI to actin. Typical simulation records both processes: (a) calcium concentration and (b) kinetics of binding of TnI to actin expressed via equilibrium constant

$$K_B = \frac{1}{K_I},$$

where

$$K_I = \frac{k_I}{k_{-I}}.$$

We used here  $K_B$  for convenience, following our publication (Mijailovich et al., 2012), so that the force- $K_B$ -force relation parallels observed force-pCa relations.

In each simulation, for a prescribed range of  $K_B$ , the steady-state isometric force can be calculated at a given SL and force- $K_B$  relation established. This relation has a similar shape as the observed tension-pCa relation and both can be described by the Hill formula as

$$F = \frac{F_o K_B^{\eta_H}}{K_{B_{50\%}}^{\eta_H} + K_B^{\eta_H}} \quad \text{and} \quad T = \frac{T_o [Ca]^{\eta_H}}{[Ca_{50\%}]^b + [Ca]^b}, \quad (\text{S3})$$

where  $F$  is average force per myosin filament from MUSICO simulations and  $T$  is observed tension;  $\eta_H$  and  $n_H$  are the Hill coefficients,  $K_{B_{50\%}}$  and  $[Ca_{50\%}]$  are the values at 50% of isometric force,  $F_o$ , or isometric tension,  $T_o$ . The relationship between tension,  $T$ , and myosin filament force,  $F$ , can be calculated from the relation  $F = T/\#$  myofilaments per unit of muscle cross-sectional area, as described in the main text. Calcium concentration is usually plotted in terms of pCa =  $-\log([Ca])$ . The parameters from fitted force-pCa relations from simulations and tension-pCa relations from the observations provide the net effect of changes in binding kinetics and CFC elasticity within confined energy landscape reflecting interaction of CFC with actin. The relationship between  $K_B$  and pCa is approximately linear over a wide range of  $K_B$  and pCa values, and this relationship can be derived from Eq. A1 in Smith and Geeves (2003). Therefore, the  $K_B$ -pCa relation can be obtained from the fits of  $F$ - $K_B$  MUSICO simulation data and  $T$ -pCa observed relations, i.e., the estimated parameters are defined by Hill equations (Eq. S3). The Hill parameters for the effects of lack of nebulin in skeletal muscle are summarized in Table S1, and Table S2 shows the parameters for the effects of various levels of titin-based passive tension in cardiac muscle as reported by Cazorla et al. (2001).

### Decrease in force and muscle stiffness with increase in thin filament compliance in nebulin-deficient actin filaments

Recent measurements of thin filament stiffness in intact mouse soleus muscle (Kiss et al., 2018) showed lower values than directly measured by Kojima et al. (1994), i.e.,  $\sim 34$  pN·nm<sup>-1</sup> in WT versus 65 pN·nm<sup>-1</sup> per 1- $\mu$ m-long filament, respectively. Part of this difference can be explained by stiffening of thin filament by the phalloidin used in the studies of Kojima et al. (Kojima et al., 1994; Kiss et al., 2018). For example, Isambert et al. (1995a) showed that phalloidin increases the persistence length of the thin filaments but clear differences in thin filament stiffness can be only roughly estimated from these measurements. On the other hand, the thin filament stiffness of 53 pN·nm<sup>-1</sup> for 1- $\mu$ m-long actin filament, estimated from the stiffness of muscle fiber from two different SLs (1.8 and 2.4  $\mu$ m) by Higuchi et al. (1995), was  $\sim 15\%$  lower than reported by Kojima et al. (1994); thus the effect of stiffening by phalloidin could be up to 15%. In nebulin-deficient soleus muscle, the reported actin stiffness is even lower, having a value of 13 pN·nm<sup>-1</sup> per 1- $\mu$ m-long filament. The observed effect of phalloidin on thin filament activation in skinned cardiac muscle (Bukatina et al., 1995) does not affect our simulation, because the experiments that we simulate did not involve phalloidin.

Kawai et al. (2018) proposed as an alternative hypothesis that the force per cross-bridge is reduced if nebulin is absent. We tested this hypothesis using MUSICO simulations to see to what degree the increases in thin filament compliance (Kiss et al., 2018) decrease isometric force, cross-bridge force, and overall muscle stiffness at full activation. The simulations showed that only  $\sim 3\%$  of the isometric drop in force can be contributed to the fourfold increase in actin filament compliance, but the muscle stiffness decreased severalfold (Fig. S2). The small decrease in tension is similar to the change of the average cross-bridge force. The same geometry and cross-bridge cycle were used in all simulations, and only the actin filament compliance was varied, including the range covering the Kojima et al. (1994) stiffness 65 pN·nm<sup>-1</sup> and the Kiss et al. (2018) measurements in intact mouse soleus muscle in WT of  $\sim 34$  and in nebulin-deficient of 14 pN·nm<sup>-1</sup> over 1- $\mu$ m-long filament. The cross-bridge and myosin filament stiffnesses are the same as displayed in the main text. The changes in muscle tension (kPa) and in overall muscle stiffness (MPa) are shown for different thin filament stiffnesses, whereas all other parameters were kept the same.

These results may seem as contradictory to the concept of “mechanical tuning” introduced by Daniel et al. (1998). The main differences between the Daniel et al. (1998) model and MUSICO are the number of myosin binding sites on actin filament, the frequency of cross-bridges bound to thin filaments, and the number of thick and thin filaments included in the simulations. The Daniel et al. (1998) simulation observed large increases in isometric force reaching a maximum when the filament compliance was  $\sim 10$  times higher than that observed by Huxley et al. (1994), Kojima et al. (1994), and Wakabayashi et al. (1994). The maximum was

much higher when the cross-bridge stiffness was larger than  $4 \text{ pN}\cdot\text{nm}^{-1}$ , i.e., where cross-bridge compliance is comparable with thin filament stiffness. It is important to note that in study by Daniel et al. (1998), the effect of mechanical tuning is most prominent when thin filament and cross-bridge compliances change within a large range of values, far exceeding the observed compliances.

In contrast, in our simulations, shown above, we used thin filament compliances that increased up to four times compared with those reported by Kojima et al. (1994) and a cross-bridge compliance of  $1.25 \text{ pN}\cdot\text{nm}^{-1}$ . For changes in compliances in this range, the change of isometric tension predicted by Daniel et al. (1998) was small and consistent with the predictions by MUSICO (Fig. S2).

### Decrease in calcium sensitivity with prospective increase in actin filament compliance in nebulin-deficient thin filaments

Chase et al. (2004) showed that the changes in compliances of thin filaments and cross-bridges strongly affect calcium sensitivity of force-pCa relations. Because the lack of nebulin could strongly increase thin filament compliance, we calculated the effect of a change of compliance in the range reported by Kiss et al. (2018) on the calcium sensitivity. The simulations show that the increase in thin filament compliances slightly decreased isometric force and calcium sensitivity (Fig. S3 A). The net change in sensitivity for three thin filament compliances is shown in Fig. S3 B. The change in sensitivity was small ( $\Delta\text{pCa}_{50} \sim 0.038$ ) when thin filament stiffness changed from  $65 \text{ pN}\cdot\text{nm}^{-1}$  reported by Kojima et al. (1994) to  $34 \text{ pN}\cdot\text{nm}^{-1}$  estimated in WT soleus muscle thin filaments from small-angle x-ray diffraction studies (Kiss et al., 2018). A similar change in sensitivity is observed between WT and Neb-KO deficient thin filaments. However, the lengths of thin filaments in Neb-KO are nonuniform and shorter than in WT; thus the net effect of the above decrease in thin filament stiffness (by a factor of 3) on the calcium sensitivity is even smaller,  $\Delta\text{pCa} = 0.025$ .

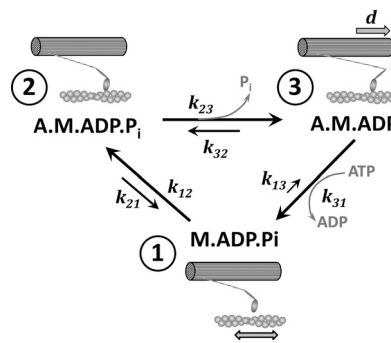


Figure S1. **The three-state model of the actomyosin cycle.** The model consists of a detached state 1 (M.ADP.Pi), weakly bound state 2 (A.M.ADP.Pi), and strongly bound post-power stroke state 3 (A.M.ADP). The transition between the detached state 1 involves binding of cross-bridges to available actin sites, forming weakly bound state 2, whereas transition from state 2 involves the phosphate released from the attached myosin head followed by lever arm displacement  $d$  to create a strongly bound state 3. Because the actomyosin cycle and the corresponding structural states of myosin head consist of at least six biochemical states, the reduction to the minimal three-state model requires grouping of transitions between A.M, A.M.ATP, M.ATP, and M.ADP.Pi states to a single transition, where forward rate is dominated by the rate of ADP release, and backward rate, i.e., reverse attachment from M.ATP to A.M.ATP, is by far slowest and can be neglected. The compounded state transition includes ADP release associated with lever arm displacement  $\delta$  to open the nucleotide pocket, ATP binding, dissociation of myosin from actin, and ATP hydrolysis step.

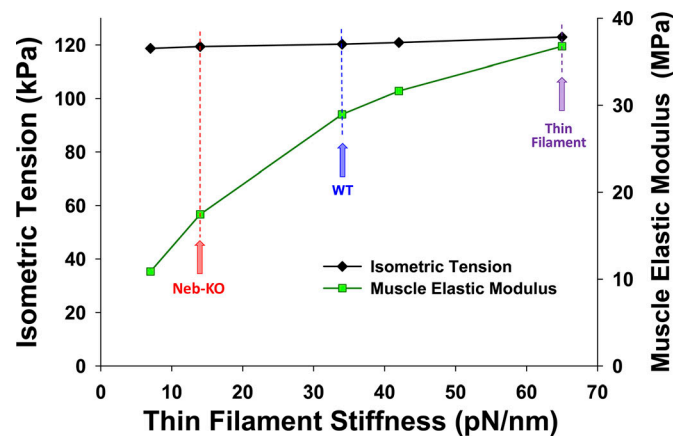


Figure S2. **MUSICO predictions of isometric tension and muscle elastic modulus over the range of thin filament stiffnesses.** The isometric tension is proportional to average force per myosin filament, interfilament lattice spacing, e.g.,  $d_{1,0}$ , and fraction of muscle cross section filled with myofibrils (Mijailovich et al., 2016). Muscle instantaneous stiffness, defined as the increases in tension after instantaneous small stretch over the amount of the stretch, is obtained from MUSICO simulations. The elastic modulus is defined as an increase in tension by an increase in strain, i.e., equal to the instantaneous stiffness over characteristic length over which the stretch is applied. Kojima et al. (1994) measurements are denoted as Thin Filament, Kiss et al. (2018) measurements for soleus muscle (control) as WT, and for nebulin-deficient as *Neb-KO*. In all calculations, the three-state cycle is used, with the same kinetic parameters as used in the main text for WT. All simulations use the same geometry of the sarcomere,  $SL = 2.5 \mu\text{m}$ , and actin filaments have uniform length of  $1.2 \mu\text{m}$ .

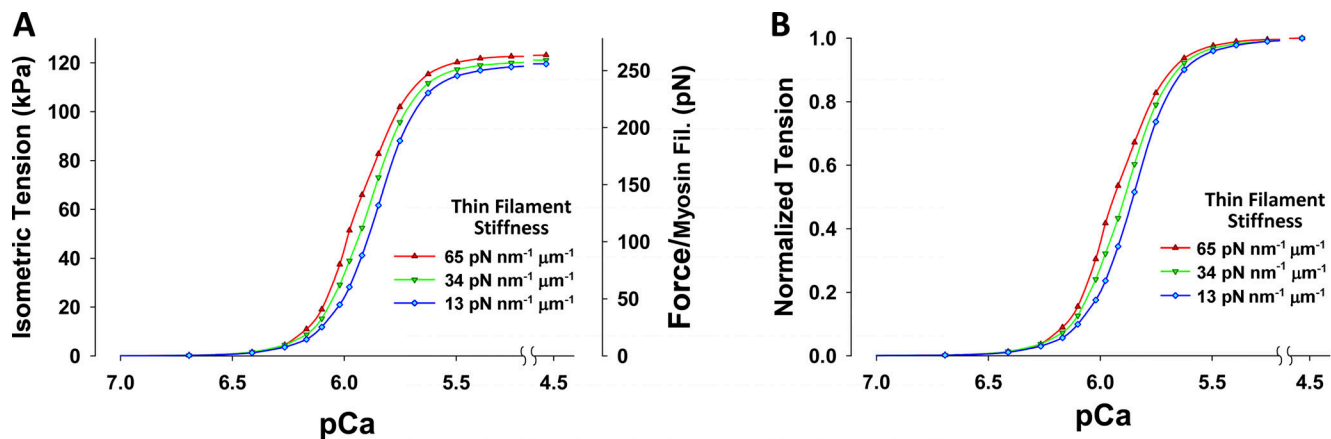


Figure S3. **The effect of thin filament stiffness on calcium sensitivity.** (A) Changes in isometric tension or force per myosin filament, and calcium sensitivity in the physiological range of calcium concentration. (B) Normalized tension or force versus calcium concentration shows net effect of change in thin filament stiffness on the calcium sensitivity. The geometry and all kinetic parameters are the same as used in simulations for WT mouse soleus muscle. The thin filament stiffness values used are as follows:  $65 \text{ pN}\cdot\text{nm}^{-1}$  observed by Kojima et al. (1994) in isolated thin filaments,  $34 \text{ pN}\cdot\text{nm}^{-1}$  estimated by Kiss et al. (2018) in mouse WT muscles, and  $13 \text{ pN}\cdot\text{nm}^{-1}$  estimated in *Neb-KO* muscles (Kiss et al., 2018).

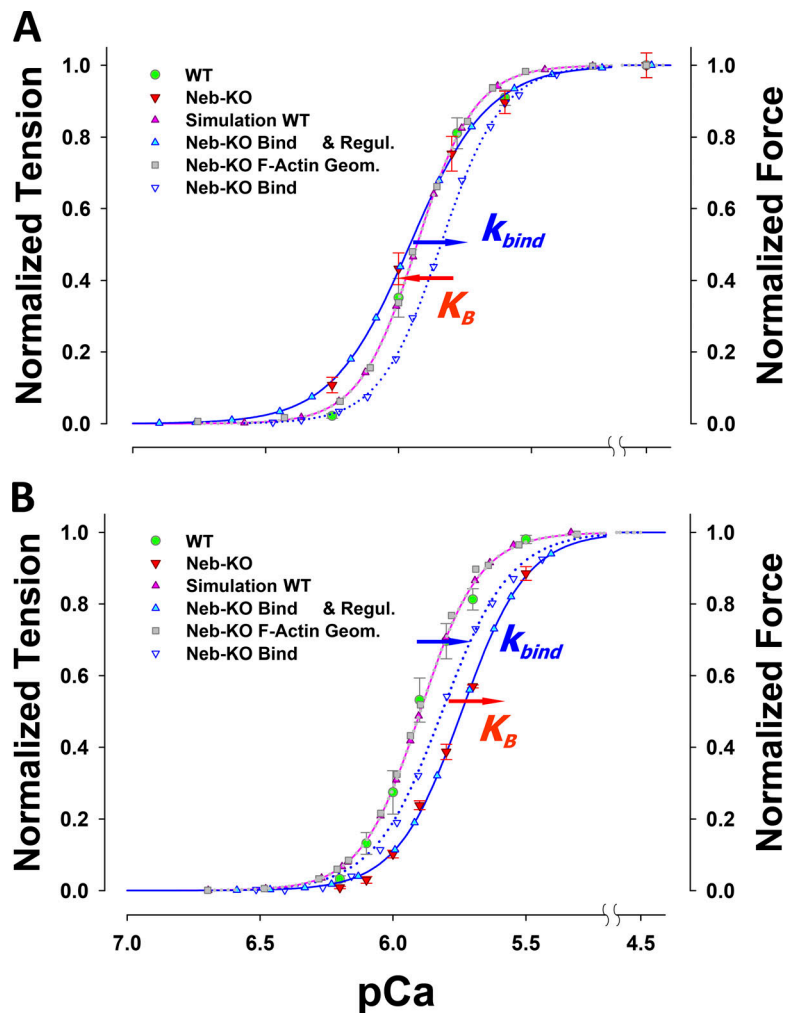


Figure S4. **Normalized force-pCa relations of WT and nebulin-deficient muscles.** The figures are adapted from Fig. 6 (B and C) for the calcium sensitivity analysis. **(A)** Predicted normalized force-pCa relation at 2.5  $\mu\text{m}$  for WT (pink triangles and line) agrees well with observations (black filled circles with bars; Witt et al., 2006). To match the tension of fully activated muscle with the nebulin-deficient muscle (blue open triangle and blue dotted line), it was necessary to decrease the affinity of myosin to regulated thin filament (i.e.,  $k_{bind}$ ) by  $\sim 2.4$ -fold. The simulations including sarcomere geometry of nebulin-deficient muscles showed lower calcium sensitivity for  $\Delta\text{pCa}_{50} = 0.0898$  (blue horizontal arrow). To match the observations, an increase in sensitivity of  $\Delta\text{pCa} \cong 0.116$  was achieved by decreasing calcium off rate from TnC, i.e., an increase in TnI detachment rate from thin filament,  $k_{-1}$  (i.e., equilibrium constant  $K_B$ ), and the predicted force-pCa relations (cyan filled triangles and blue line) then agreed well with observations (red triangles with bars). **(B)** Predicted force-pCa relation at 2.0  $\mu\text{m}$  for WT (pink triangles and line) agrees well with data of Chandra et al. (2009) (green filled circles with bars). Here also, at full activation, nebulin-deficient muscle binding affinity (i.e.,  $k_{bind}$ ) has to be decreased, in this case 3.3-fold, so that predicted force matches observed tension levels (blue open triangle and blue dotted line vs. red triangles with bars). In this case, the predictions also showed lower sensitivity for  $\Delta\text{pCa}_{50} = 0.0827$  (blue horizontal arrow), but this decrease was not sufficient to match Neb-KO observations. Thus, to match Chandra et al. (2009) data, the additional decrease in sensitivity of  $\Delta\text{pCa} \cong 0.075$  was achieved by increasing calcium off rate from TnC used in the WT, i.e., a decrease of  $k_i$  (i.e., equilibrium constant  $K_B$ ), and the predicted force-pCa relations (cyan filled triangles and blue line) then agreed well with observations (red triangles with bars).

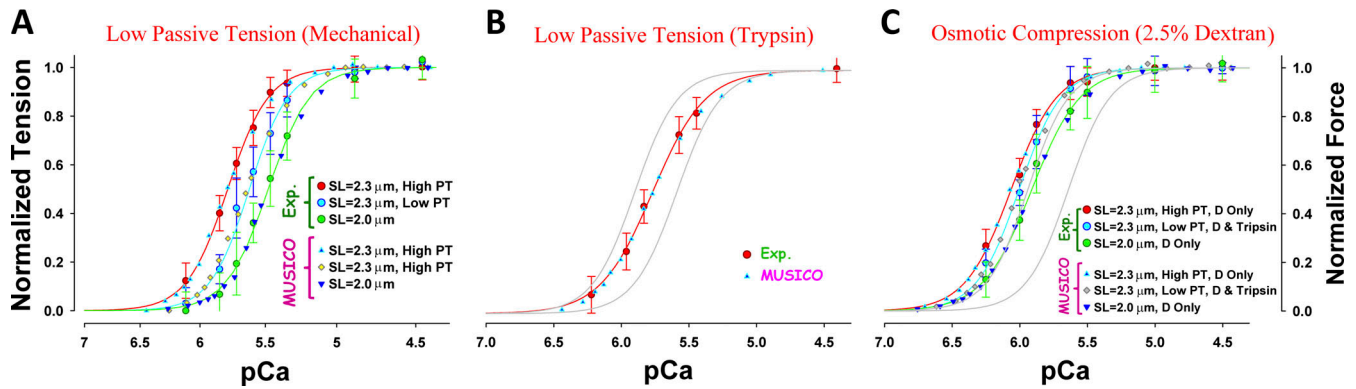


Figure S5. **Normalized force-pCa relations at high and low titin passive tension.** Normalized force-pCa relations showing the effect of changes in titin-based passive force in cardiac muscles. The figures are adapted from Fig. 7 (B and C) for the calcium sensitivity analysis. Observed force-pCa relations (symbols with bars) are compared with MUSICO predictions (symbols and lines) at SL 2.0 and 2.3  $\mu\text{m}$  and at HPT and LPT. **(A)** Predicted normalized force-pCa relation at 2.3  $\mu\text{m}$  at HPT and at LPT achieved by stretching myocytes to SL 2.5  $\mu\text{m}$ , holding, releasing to SL of 2.3  $\mu\text{m}$ , and then activating (mechanical protocol) or at SL = 2.0  $\mu\text{m}$ . **(B)** LPT achieved by trypsin treatment of the cells at SL = 2.3  $\mu\text{m}$ . **(C)** The effect of osmotic compression (2.5% dextran). For reference, thin gray lines in B and C show force-pCa relations at 2.3  $\mu\text{m}$  SL at HPT and at 2.0  $\mu\text{m}$  SL from A.

Table S1. **Effects of nebulin deficiency on calcium sensitivity in skeletal muscle**

SL	Protocols	Active force	$d_{1,0}$	$n_H$	$\eta_H$	$n_H/\eta_H$	$pCa_{50}$	Log	$\Delta pCa_{50}$	$\Delta \text{Log}$
$\mu\text{m}$		pN/MyoF	nm					$K_{B_{50}}$		$K_{B_{50}}$
<a href="#">Witt et al. (2006)</a>										
2.5	WT	262.61	37.363	4.0010	1.42390	2.8099	5.9309	1.5231		
2.5	Neb-KO (Geom)	199.51	37.363	4.0662	1.46824	2.7694	5.9465	1.5004	0.0156	0.0227
2.5	Neb-KO	120.17	37.363	2.9564	1.34030	2.2058	5.9572	1.7788	0.0263	-0.2556
<a href="#">Chandra et al. (2009)</a>										
2.0	WT	179.10	41.774	3.8857	1.3942	2.7870	5.8972	1.7215		
2.0	Neb-KO (Geom)	181.96	41.774	3.8857	1.4355	2.7069	5.8972	1.7061	0.0000	0.0154
2.0	Neb-KO	80.48	41.774	3.5469	1.2134	2.9231	5.7414	1.9520	-0.1558	-0.2305

Comparison of Hill coefficients and  $\Delta pCa_{50}$  at two SLs: SL = 2.5  $\mu\text{m}$  (Witt et al., 2006) and SL = 2.0  $\mu\text{m}$  (Chandra et al., 2009).  $n_H$  indicates Hill coefficient in force-pCa relations, and  $\eta_H$  in force- $K_B$  relations;  $\Delta pCa_{50}$  is difference between  $pCa_{50}$  of Neb KO and  $pCa_{50}$  of WT, and  $\Delta \text{log}(K_{B_{50\%}})$  is difference between  $\text{log}(K_{B_{50\%}})$  of Neb KO and of WT. Note that  $pCa_{50}$  increase and  $\text{log}(K_{B_{50\%}})$  decrease are associated with increased calcium sensitivity and the opposite trend is rooted in their definition. Consequently, the differences  $\Delta pCa_{50}$  and  $\Delta \text{log}(K_{B_{50\%}})$  will have opposite signs; thus for comparisons we used  $-\Delta \text{log}(K_{B_{50\%}})$ . Geom, sarcomere geometry of Neb-KO only.



Table S2. **Effects of passive tension, trypsin, and dextran on calcium sensitivity in cardiac muscle**

SL	Protocols	Active force	Passive force	$d_{1,0}$	$n_H$	$\eta_H$	$n_H/\eta_H$	$pCa_{50}$	Log	$\Delta pCa_{50}$	$\Delta Log$
$\mu m$		pN/MyoF	pN/MyoF	nm					$K_{B_{50\%}}$		$K_{B_{50}}$
2	LPT	98.65	1.93	42.856	2.8656	1.3800	2.0765	5.6524	2.5048		
2.3	LPT (Mech)	101.31	5.46	40.902	2.8223	1.2280	2.2983	5.7932	2.3336	0.1408	0.1712
2.3	HPT (Mech)	110.21	27.95	40.902	2.7663	1.2780	2.1646	5.9367	2.3080	0.2843	0.1969
2.3	LPT (Trypsin)	106.36	5.46	43.668	2.3140	1.1470	2.0174	5.8128	2.3051	0.1604	0.1998
2	LPT + Dextran	104.11	1.29	35.599	2.4000	1.3320	1.8018	5.9100	2.5246		
2.3	LPT (Mech) + Dextran	112.14	7.07	35.003	2.7500	1.3619	2.0192	6.0039	2.2925	0.0939	0.2321
2.3	HPT + Dextran	117.6	27.95	35.003	2.5500	1.3020	1.9585	6.0628	2.1965	0.1528	0.3281

Dextran, reduced filament spacing by osmotic compression with 2.5% dextran in skinned muscle preparation; Mech, mechanical protocol; Trypsin, skinned muscle preparations in which the titin had been degraded by 0.25 mg/ml trypsin for 25 min at 25°C.  $n_H$  indicates Hill coefficient in force–pCa relations, and  $\eta_H$  in force– $K_B$  relations;  $\Delta pCa_{50}$  is difference between  $pCa_{50}$  at SL 2.3 and  $pCa_{50}$  at 2.0  $\mu m$ , and  $\Delta Log(K_{B_{50\%}})$  is difference between  $\log(K_{B_{50\%}})$  at SL 2.3 and 2.0  $\mu m$ . Because  $pCa_{50}$  increase and  $\log(K_{B_{50\%}})$  decrease are associated with increased calcium sensitivity and the opposite trend is rooted in their definition, for comparisons of  $\Delta pCa_{50}$  and  $\Delta \log(K_{B_{50\%}})$  we used  $-\Delta \log(K_{B_{50\%}})$ .

## References

- Bukatina, A.E., F. Fuchs, and P.W. Brandt. 1995. Thin filament activation by phalloidin in skinned cardiac muscle. *J. Mol. Cell. Cardiol.* 27:1311–1315. [https://doi.org/10.1016/S0022-2828\(05\)82393-4](https://doi.org/10.1016/S0022-2828(05)82393-4)
- Cazorla, O., Y. Wu, T.C. Irving, and H. Granzier. 2001. Titin-based modulation of calcium sensitivity of active tension in mouse skinned cardiac myocytes. *Circ. Res.* 88:1028–1035. <https://doi.org/10.1161/hh1001.090876>
- Chandra, M., R. Mamidi, S. Ford, C. Hidalgo, C. Witt, C. Ottenheijm, S. Labeit, and H. Granzier. 2009. Nebulin alters cross-bridge cycling kinetics and increases thin filament activation: a novel mechanism for increasing tension and reducing tension cost. *J. Biol. Chem.* 284:30889–30896. <https://doi.org/10.1074/jbc.M109.049718>
- Chase, P.B., J.M. Macpherson, and T.L. Daniel. 2004. A spatially explicit nanomechanical model of the half-sarcomere: myofilament compliance affects Ca(2+) activation. *Ann. Biomed. Eng.* 32:1559–1568. <https://doi.org/10.1114/B:ABME.0000049039.89173.08>
- Daniel, T.L., A.C. Trimble, and P.B. Chase. 1998. Compliant realignment of binding sites in muscle: transient behavior and mechanical tuning. *Biophys. J.* 74:1611–1621. [https://doi.org/10.1016/S0006-3495\(98\)77875-0](https://doi.org/10.1016/S0006-3495(98)77875-0)
- Duke, T.A. 1999. Molecular model of muscle contraction. *Proc. Natl. Acad. Sci. USA.* 96:2770–2775. <https://doi.org/10.1073/pnas.96.6.2770>
- Higuchi, H., T. Yanagida, and Y.E. Goldman. 1995. Compliance of thin filaments in skinned fibers of rabbit skeletal muscle. *Biophys. J.* 69:1000–1010. [https://doi.org/10.1016/S0006-3495\(95\)79975-1](https://doi.org/10.1016/S0006-3495(95)79975-1)
- Hunt, A.J., F. Gittes, and J. Howard. 1994. The force exerted by a single kinesin molecule against a viscous load. *Biophys. J.* 67:766–781. [https://doi.org/10.1016/S0006-3495\(94\)80537-5](https://doi.org/10.1016/S0006-3495(94)80537-5)
- Huxley, H.E., A. Stewart, H. Sosa, and T. Irving. 1994. X-ray diffraction measurements of the extensibility of actin and myosin filaments in contracting muscle. *Biophys. J.* 67:2411–2421. [https://doi.org/10.1016/S0006-3495\(94\)80728-3](https://doi.org/10.1016/S0006-3495(94)80728-3)
- Isambert, H., P. Venier, A.C. Maggs, A. Fattoum, R. Kassab, D. Pantaloni, and M.F. Carlier. 1995a. Flexibility of actin filaments derived from thermal fluctuations. Effect of bound nucleotide, phalloidin, and muscle regulatory proteins. *J. Biol. Chem.* 270:11437–11444. <https://doi.org/10.1074/jbc.270.19.11437>
- Kawai, M., T.S. Karam, J. Kolb, L. Wang, and H.L. Granzier. 2018. Nebulin increases thin filament stiffness and force per cross-bridge in slow-twitch soleus muscle fibers. *J. Gen. Physiol.* 150:1510–1522. <https://doi.org/10.1085/jgp.201812104>
- Kiss, B., E.-J. Lee, W. Ma, F.W. Li, P. Tonino, S.M. Mijailovich, T.C. Irving, and H.L. Granzier. 2018. Nebulin stiffens the thin filament and augments cross-bridge interaction in skeletal muscle. *Proc. Natl. Acad. Sci. USA.* 115:10369–10374. <https://doi.org/10.1073/pnas.1804726115>
- Kojima, H., A. Ishijima, and T. Yanagida. 1994. Direct measurement of stiffness of single actin filaments with and without tropomyosin by in vitro nanomanipulation. *Proc. Natl. Acad. Sci. USA.* 91:12962–12966. <https://doi.org/10.1073/pnas.91.26.12962>
- Kramers, H.A. 1940. Brownian motion in a field of force and the diffusion model of chemical reactions. *Physica.* 7:284–304. [https://doi.org/10.1016/S0031-8914\(40\)90098-2](https://doi.org/10.1016/S0031-8914(40)90098-2)
- Mijailovich, S.M., O. Kayser-Herold, X. Li, H. Griffiths, and M.A. Geeves. 2012. Cooperative regulation of myosin-S1 binding to actin filaments by a continuous flexible Tm-Tn chain. *Eur. Biophys. J.* 41:1015–1032. <https://doi.org/10.1007/s00249-012-0859-8>
- Mijailovich, S.M., O. Kayser-Herold, B. Stojanovic, D. Nedic, T.C. Irving, and M.A. Geeves. 2016. Three-dimensional stochastic model of actin-myosin binding in the sarcomere lattice. *J. Gen. Physiol.* 148:459–488. <https://doi.org/10.1085/jgp.201611608>
- Papoulis, A. 1991. *Probability, Random Variables, and Stochastic Processes*. McGraw-Hill, New York, NY.
- Smith, D.A., and M.A. Geeves. 2003. Cooperative regulation of myosin-actin interactions by a continuous flexible chain II: actin-tropomyosin-troponin and regulation by calcium. *Biophys. J.* 84:3168–3180. [https://doi.org/10.1016/S0006-3495\(03\)70041-1](https://doi.org/10.1016/S0006-3495(03)70041-1)
- Smith, D.A., and S.M. Mijailovich. 2008. Toward a unified theory of muscle contraction. II: predictions with the mean-field approximation. *Ann. Biomed. Eng.* 36:1353–1371. <https://doi.org/10.1007/s10439-008-9514-z>
- Wakabayashi, K., Y. Sugimoto, H. Tanaka, Y. Ueno, Y. Takezawa, and Y. Amemiya. 1994. X-ray diffraction evidence for the extensibility of actin and myosin filaments during muscle contraction. *Biophys. J.* 67:2422–2435. [https://doi.org/10.1016/S0006-3495\(94\)80729-5](https://doi.org/10.1016/S0006-3495(94)80729-5)
- Witt, C.C., C. Burkart, D. Labeit, M. McNabb, Y. Wu, H. Granzier, and S. Labeit. 2006. Nebulin regulates thin filament length, contractility, and Z-disk structure in vivo. *EMBO J.* 25:3843–3855. <https://doi.org/10.1038/sj.emboj.7601242>